Supplemental Information: Non-trivial role of interlayer cation states in iron-based superconductors

Daniel Guterding,[1, *] Harald O. Jeschke,[1] I. I. Mazin,[2] J. K. Glasbrenner,[3, †] E. Bascones,[4] and Roser Valentí[1]

[1]*Institut für Theoretische Physik, Goethe-Universität Frankfurt,*
Max-von-Laue-Straße 1, 60438 Frankfurt am Main, Germany
[2]*Code 6393, Naval Research Laboratory, Washington, DC 20375, USA*
[3]*National Research Council/Code 6393, Naval Research Laboratory, Washington, DC 20375, USA*
[4]*Instituto de Ciencia de Materiales de Madrid, ICMM-CSIC, Cantoblanco, 28049 Madrid, Spain*

I. METASTABILITY OF MAGNETIC STATES WITH DIFFERENT ORDERED MOMENTS IN YFe_2Ge_2

We analyzed the energies of different magnetic configurations in YFe_2Ge_2 using the FPLO density functional theory code[1] with a GGA exchange-correlation functional[2], following Refs. 3–5. We investigate the GGA+U ordered moment of YFe_2Ge_2 as a function of the Fe-Ge bond length, starting with $U = 0$. For the magnetic order we choose ferromagnetic arrangement within the iron plane and antiferromagnetic stacking along the c-axis. We find that YFe_2Ge_2 shows a peculiar metastability of ordered magnetic states with ordered moments of $m \sim 1\mu_B$ (low moment) and $m \sim 2\mu_B$ (high moment). The ground state for small Fe-Ge bond lengths has an ordered moment of about $m \sim 1\mu_B$, while the $m \sim 2\mu_B$ state can be stabilized for larger Fe-Ge bond lenghts. The results are summarized in Fig. 1. Note that some of the solutions initialized as high moment actually converged to a low moment solution.

Furthermore, we investigated the influence of Coulomb repulsion on the Fe $3d$ orbitals. We find that even a tiny Coulomb repulsion $U = 0.25$ eV is sufficient to make the high moment compete for the global energy minimum. The
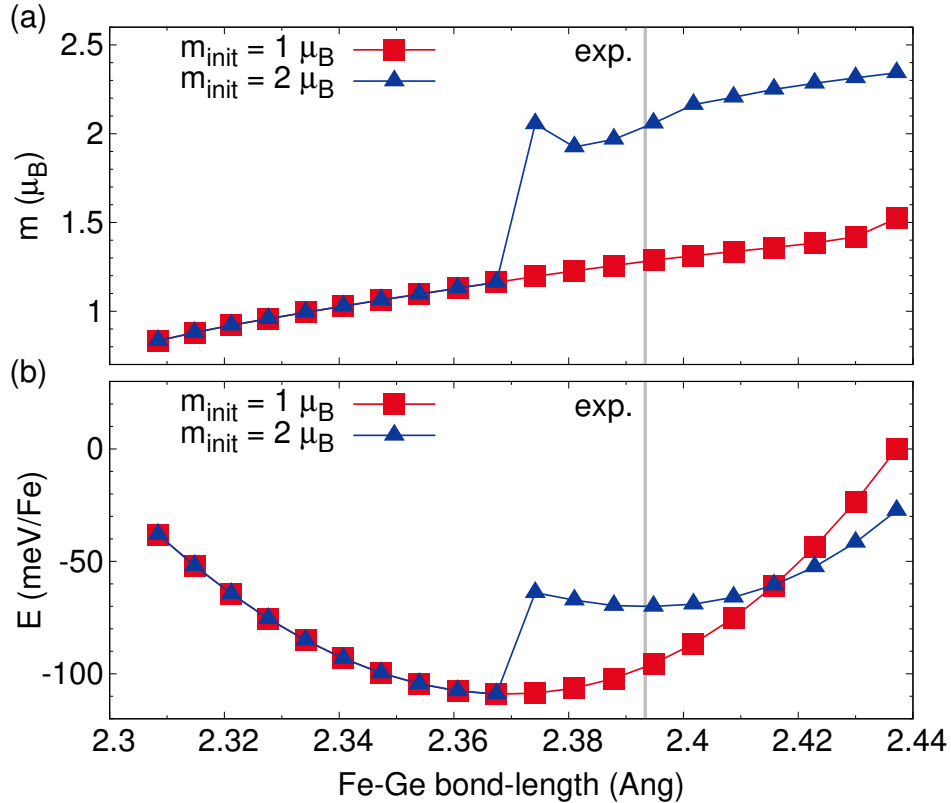
FIG. 1. (a) Magnetic moment versus Fe-Ge bond length and (b) total energy versus Fe-Ge bond length for YFe_2Ge_2. All calculations were performed with GGA xc-functional. The red curve was generated from ferromagnetic initial configurations within the Fe plane with a moment of $1\mu_B$ per Fe. The ferromagnetic planes were stacked antiferromagnetically in the c-direction. Calculations with an initial magnetic moment of $2\mu_B$ per Fe result in the blue curve. The vertical grey line marks the experimental Fe-Ge bond-length.
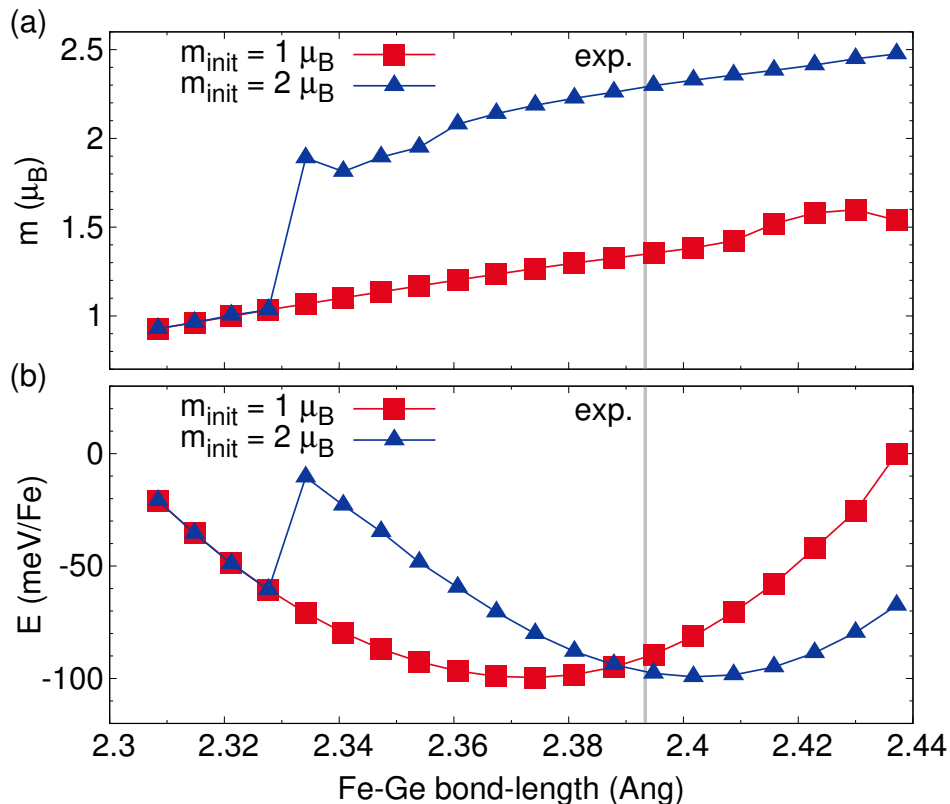
FIG. 2. (a) Magnetic moment versus Fe-Ge bond length and (b) total energy versus Fe-Ge bond length for YFe_2Ge_2. All calculations were performed with GGA+U xc-functional using $U = 0.25$ eV. The red curve was generated from ferromagnetic initial configurations within the Fe plane with a moment of $1\mu_B$ per Fe. The ferromagnetic planes were stacked antiferromagnetically in the c-direction. Calculations with an initial magnetic moment of $2\mu_B$ per Fe result in the blue curve. The vertical grey line marks the experimental Fe-Ge bond-length.

results for this calculation are summarized in Fig. 2. Note that a larger Coulomb repulsion also shifts the minimum in the energy for the high-moment solutions to larger Fe-Ge bond lengths.

The metastability of low- and high-moment solutions lead us to the investigation of the germanide compounds within the extended Stoner formalism.

II. METASTABILITY OF MAGNETIC STATES WITH DIFFERENT ORDERED MOMENTS IN MgFeGe

Using the Wien2k code and otherwise comparable calculation setup we also investigated the energy of the low- and high-moment solution in MgFeGe as a function of the Ge height. Depending on the Ge height, either the low- or the high-spin solution is stable, and the other solution manifests itself as a shoulder (inflection point) in the $E(M)$ curve. This behavior is shown in Fig. 3, which shows the values of the magnetic moment M at the energy minimum and the inflection point as a function of the Ge z-position.

III. EXTENDED STONER MODEL

In the extended Stoner calculation we follow Ref. 6. The extended Stoner theory determines whether the paramagnetic state of a material is stable against ferromagnetism.

Within the extended Stoner theory the total magnetization energy can be written as Eq. 1, where m is the magnetization and $\bar{N}(m)$ is the density of states averaged between the Fermi levels of the spin-up and the spin-down channels. In the limit of $m \to 0$ the effective Stoner DOS is simply the total DOS at the Fermi level. For all other moments m the effective Stoner DOS is the average total DOS within an increasingly large energy window around the Fermi
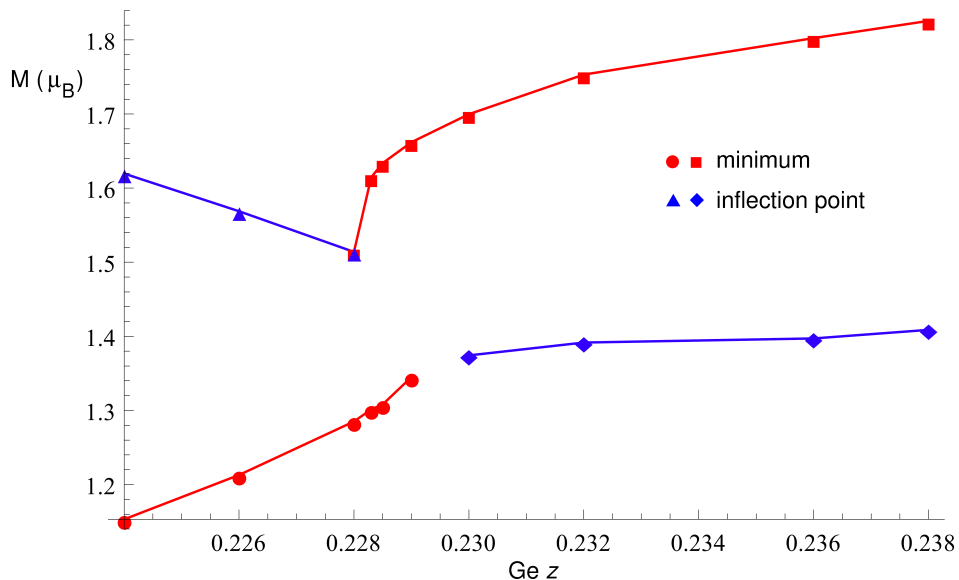
FIG. 3. Magnetic moment M at the minimum and the inflection point of the $E(M)$ curve from fixed-moment calculations in MgFeGe as a function of the Ge z-poition (Ge height). The energy minimum changes from the low-spin to the high-spin solution when Ge height is increased beyond a certain value. Lines are guides to the eye.

energy. The density of states is evaluated within the rigid-band approximation starting from the paramagnetic state.

$$E(m) = \frac{1}{2} \int_0^m \frac{m'dm'}{\bar{N}(m')} - \frac{Im^2}{4} \tag{1}$$

The first term is the one-electron energy, because the change in energy for a single electron upon generating a moment m is half the energy difference $\Delta(m)$ between the Fermi levels of the spin-up and spin-down channels. Using $\Delta(m)\bar{N}(m) = m$ one obtains Eq. 2. Integrating this expression one obtains the first term in Eq. 1.

$$\frac{dE}{dm} = \frac{\Delta(m)}{2} = \frac{m}{2\bar{N}(m)} \tag{2}$$

The second term is the so-called Stoner parameter, which parametrizes the ferromagnetic exchange-interactions between electrons in an averaged form.

Now we derive the conditions under which the paramagnetic state is unstable towards ferromagnetism. We start by finding the extrema in the energy for Eq. 1. These are given by Eq. 3.

$$0 \stackrel{!}{=} \frac{dE}{dm} = \bar{N}(m)^{-1} - I \tag{3}$$

Next we find the condition under which this extremum is a minimum in the magnetization energy. It is given by Eq. 4, where we used $I = \bar{N}(m)^{-1}$.

$$0 \stackrel{!}{<} \frac{d^2E}{dm^2} = \frac{1}{2\bar{N}(m)} - m\frac{d\bar{N}(m)/dm}{2\bar{N}(m)^2} - \frac{I}{2} = -m\frac{d\bar{N}(m)/dm}{2\bar{N}(m)^2} \tag{4}$$

As all moments m and effective densities of states are positive, the resulting condition is $0 > d\bar{N}(m)/dm$.

Combining Eqs. 3 and 4 we find that the paramagnetic state is unstable towards ferromagnetism if the conditions $1 = \bar{N}(m)I$ and $0 > d\bar{N}(m)/dm$ are fullfilled for the same value of m.

The Stoner parameter I can be obtained from fixed-moment DFT calculations by inserting the DFT energies for $E(m)$ into Eq. 1, using the paramagnetic DFT density of states to calculate $\bar{N}(m)$ and performing a numerical optimization to obtain the value of I on the parabolic term in Eq. 1. The effective Stoner parameter I was calculated from a fit to DFT total energies of ferromagnetic configurations with a moment of up to 3 μ_B per iron site. All calculations for the Stoner analysis were converged using 20^3 k-point grids.

The results are shown in Fig. 4. The values for the Stoner parameters are 1.331 eV ($RbFe_2As_2$ in YFe_2Ge_2 structure), 1.388 eV (YFe_2Ge_2), 1.392 eV (NaFeAs in MgFeGe structure) and 1.435 eV (MgFeGe). Note that the fit is good in the high moment region. The deviation for low moments probably originates from an admixture of non-Fe states, which increases the effective Stoner parameter. This would also explain why the fit is generally worse for germanide compounds, where also a significant amount of interlayer cation states is at the Fermi level. As we use extended Stoner theory only as a qualitative tool, these discrepancies are of minor importance.
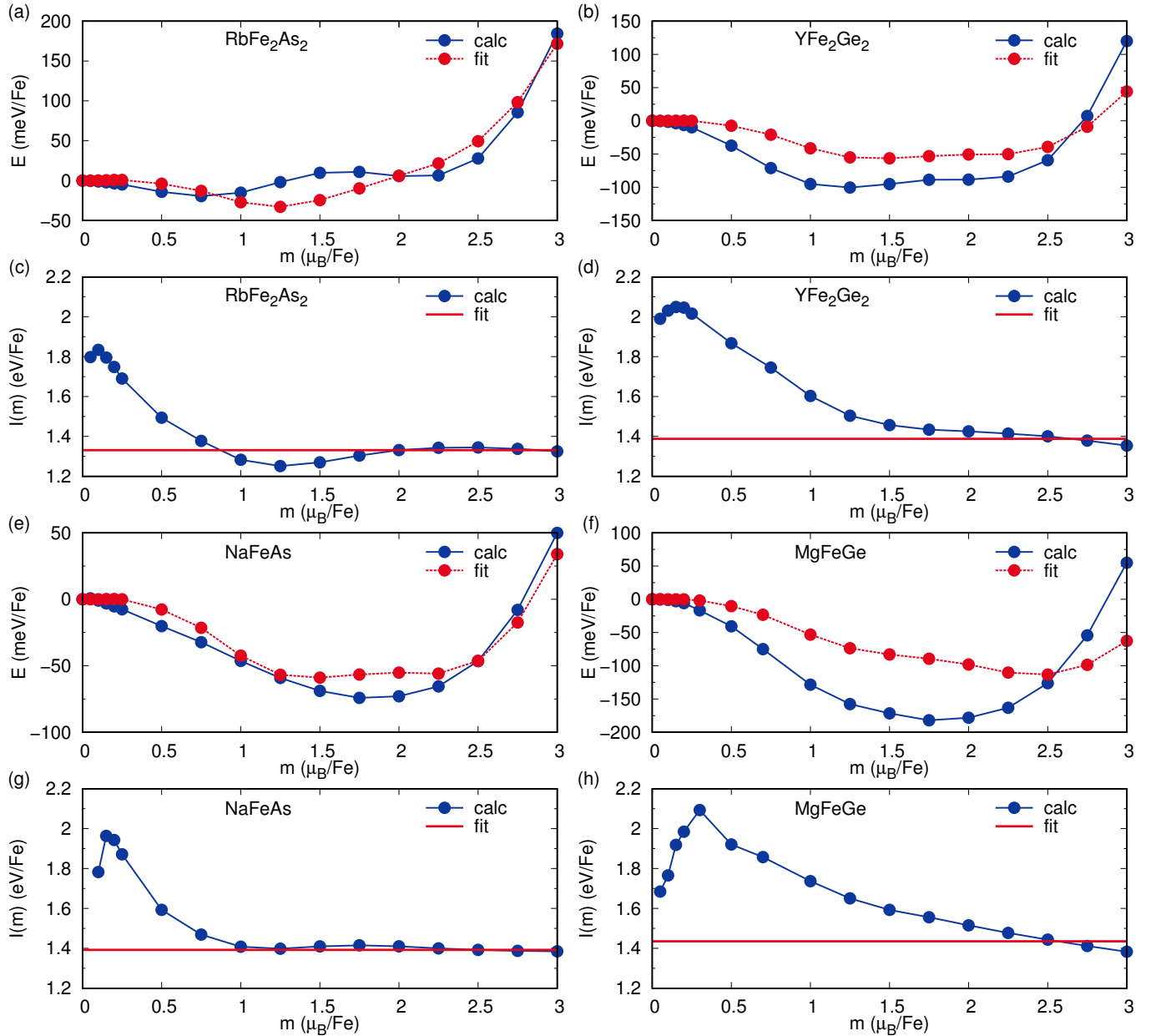
FIG. 4. (a),(b),(e),(f) Fit of Eq. 1 to the fixed-moment energies calculated from DFT. (c),(d),(g),(h) Same data as in (a),(b),(e),(f) after subtracting the one-electron energies (first term in Eq. 1) and dividing by $-m^2/4$.

IV.   DETAILS ON CALCULATION OF HEISENBERG EXCHANGE PARAMETERS

We calculate the magnetic exchange interactions based on a $2 \times 2 \times 1$ supercell containing eight Fe atoms. This leads to 17 inequivalent magnetic configurations for the *122-compounds* and 13 inequivalent configurations for the *111-compounds*. We used 8^3 k-point grids for converging these magnetic calculations. The Heisenberg exchange couplings were extracted by mapping DFT total energies of all inequivalent magnetic configurations to a classical Heisenberg model for each composition.

V.   ELECTRONIC STRUCTURE FOR VCA INTERPOLATION BETWEEN NaFeAs AND MgFeGe

We investigate the changes in electronic structure when continuously turning MgFeGe into NaFeAs using the virtual crystal approximation, while keeping all structural parameters constant. The electronic bandstructures with orbital weights are shown in Figs. 5, 6 and 7.

The flattening of bands described in the main text can be seen in Fig. 5, where the Fe d_{xz} states at the X-point are lowered almost to the Fermi level in MgFeGe and the corresponding band becomes very flat. In the same figure one can see that the Fe d_{xy} states in turn increase their bandwidth when going from NaFeAs to MgFeGe, for example by comparing the path segment M-Γ. Fig. 7 shows that the cation states are lowered very much in energy, for example at the M-point. Furthermore, their weight at the lower end of the energy range shown increases when going from NaFeAs to MgFeGe.
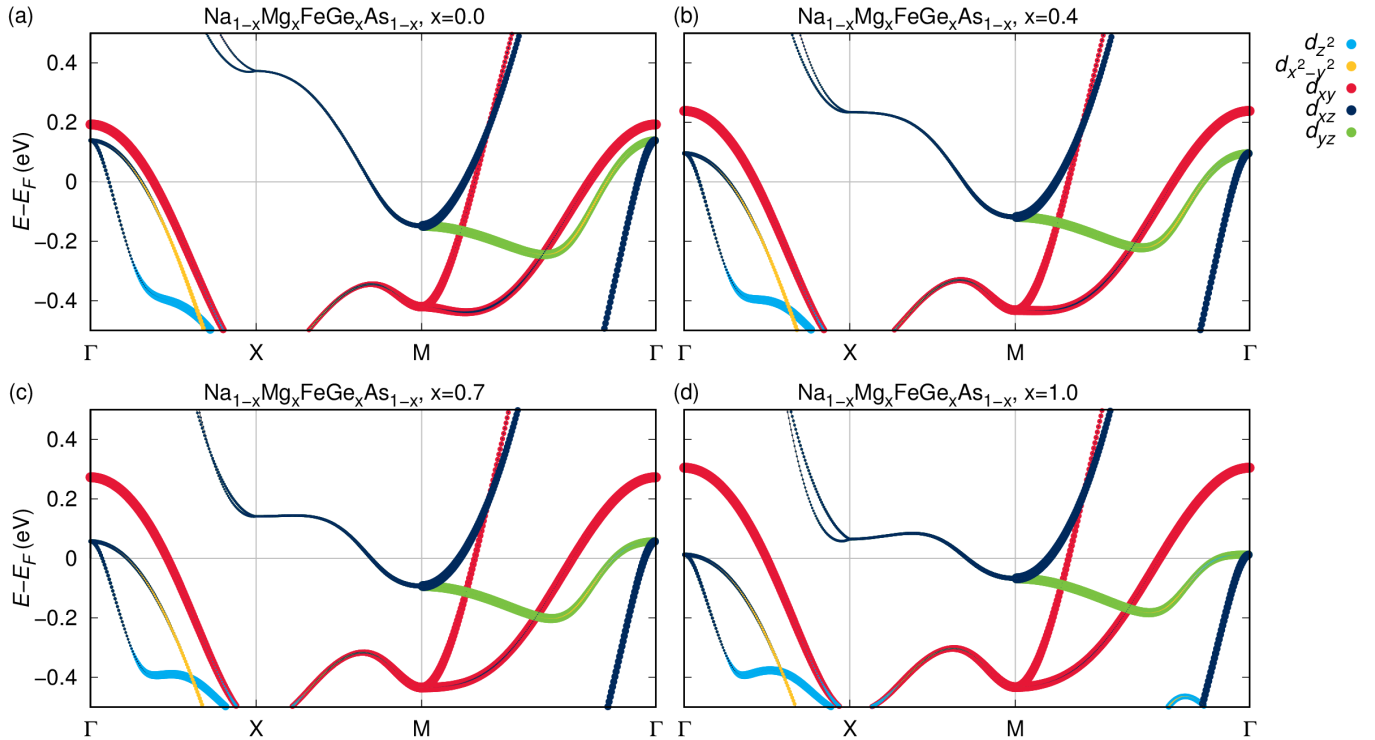
FIG. 5. Electronic bandstructure for the VCA interpolation between NaFeAs and MgFeGe. Colors indicate the weights of Fe $3d$ orbitals.
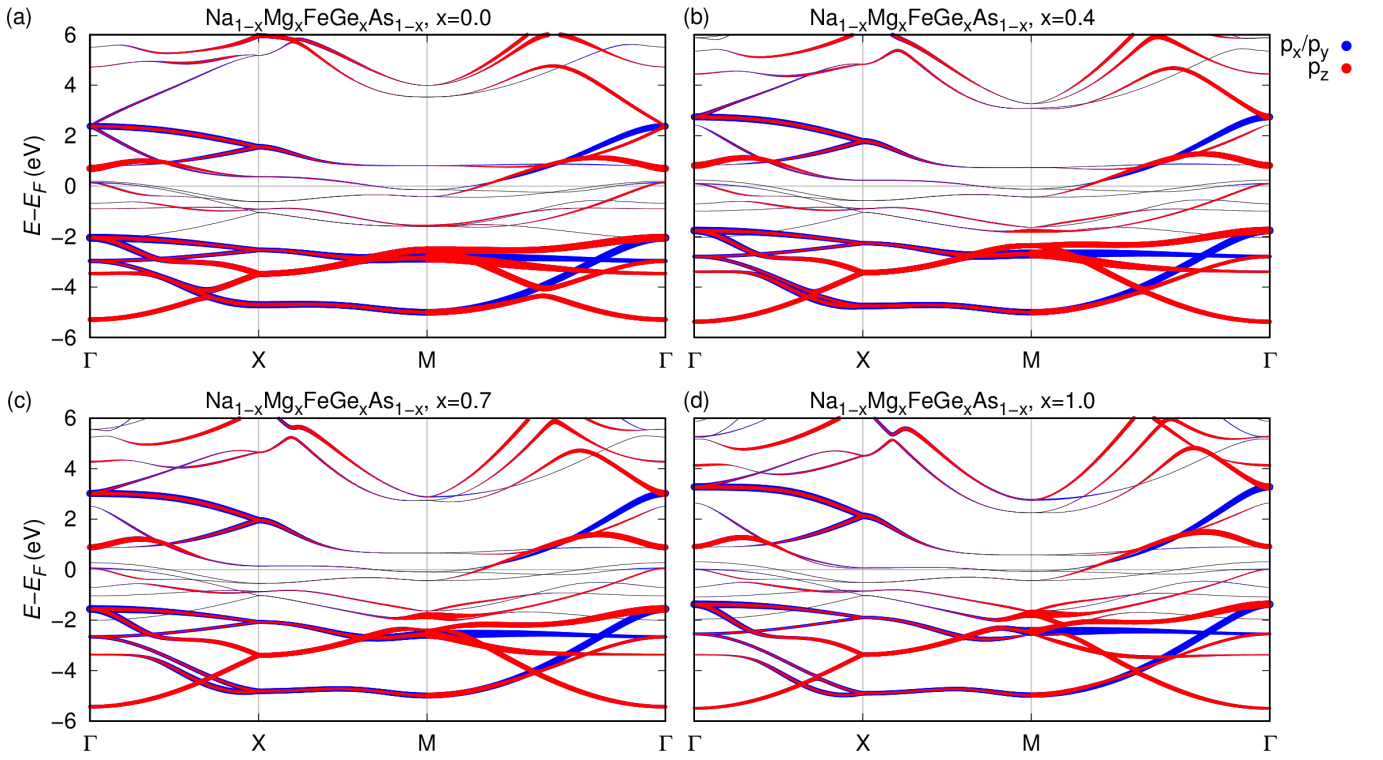
FIG. 6. Electronic bandstructure for the VCA interpolation between NaFeAs and MgFeGe. Colors indicate the weights of As/Ge $4p$ orbitals.
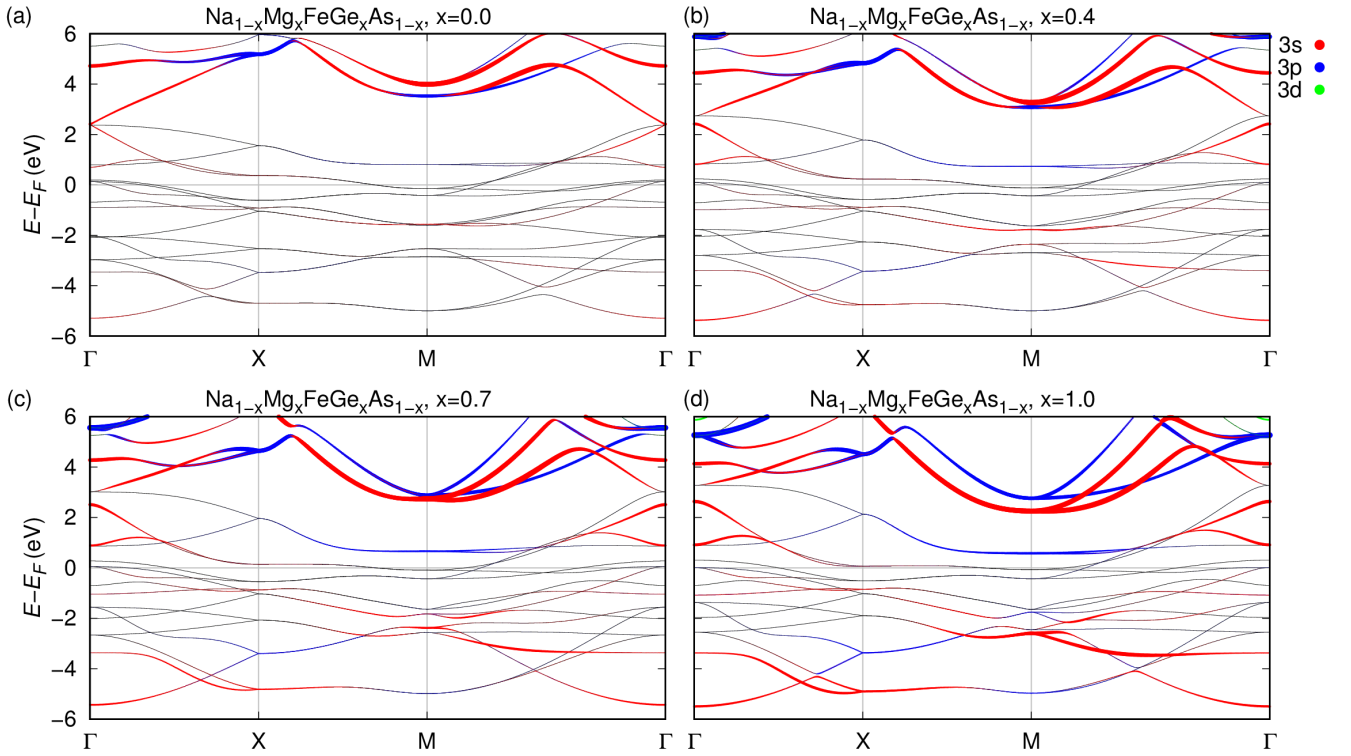
FIG. 7. Electronic bandstructure for the VCA interpolation between NaFeAs and MgFeGe. Colors indicate the weights of Na/Mg $3s$, $3p$ and $3d$ orbitals.

VI. ELECTRONIC STRUCTURE FOR VCA INTERPOLATION BETWEEN RbFe$_2$As$_2$ AND YFe$_2$Ge$_2$

We investigate the changes in electronic structure when continuously turning YFe$_2$Ge$_2$ into RbFe$_2$As$_2$ using the virtual crystal approximation, while keeping all structural parameters constant. The VCA calculation is carried out starting from strontium on the yttrium/rubidium site. The electronic bandstructures with orbital weights are shown in Figs. 8, 9 and 10.

The flattening of bands described in the main text can be seen in Fig. 8. Here it is most pronounced as a flattening of Fe $3d_{xz/yz}$ states on the M-Γ path segment. The effect of cation substitution on the position of the As/Ge $4p_z$ at the Γ-point is very strong here, as can be seen in Fig. 9 at the lower end of the energy window. Fig. 10 shows that the cation states are lowered very much in energy, for example at the Γ-point. Furthermore, their weight at the Fermi level strongly increases when going from RbFe$_2$As$_2$ to YFe$_2$Ge$_2$.
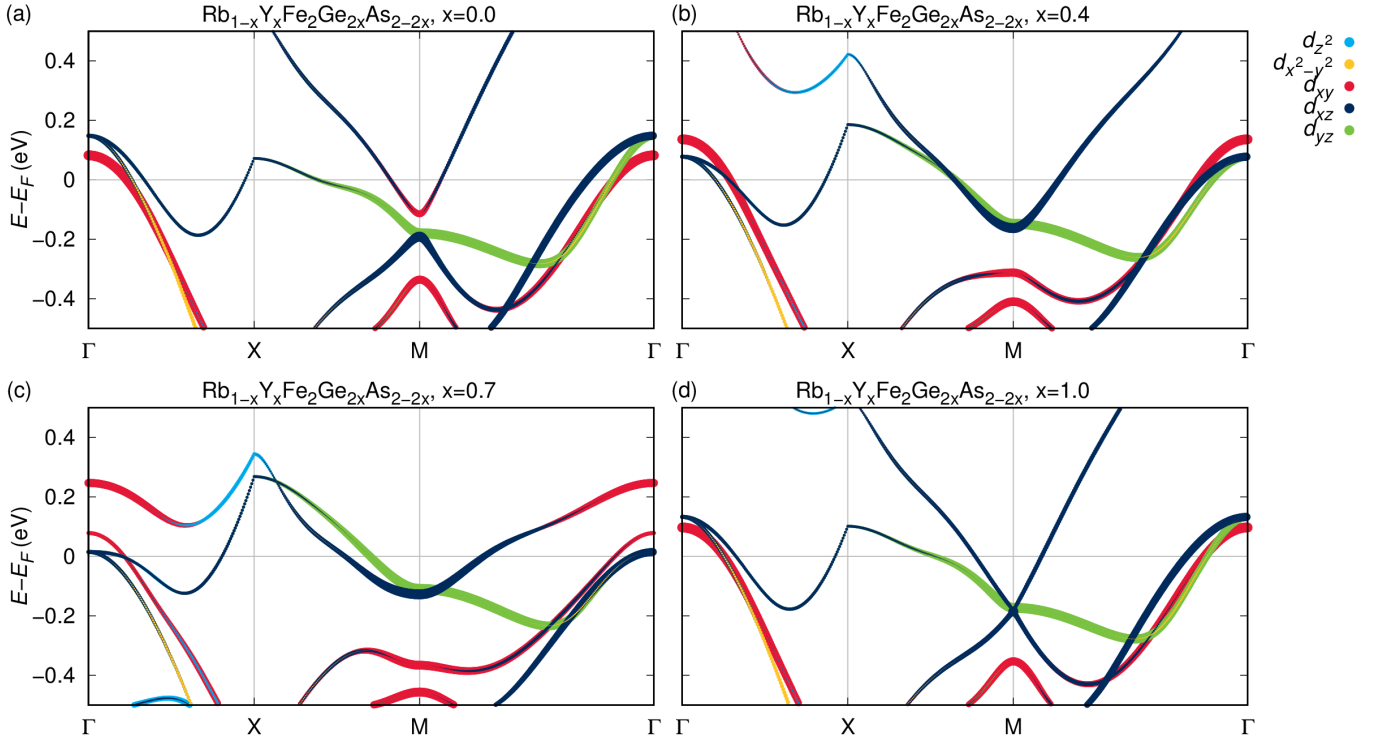
FIG. 8. Electronic bandstructure for the VCA interpolation between RbFe$_2$As$_2$ and YFe$_2$Ge$_2$. Colors indicate the weights of Fe $3d$ orbitals.
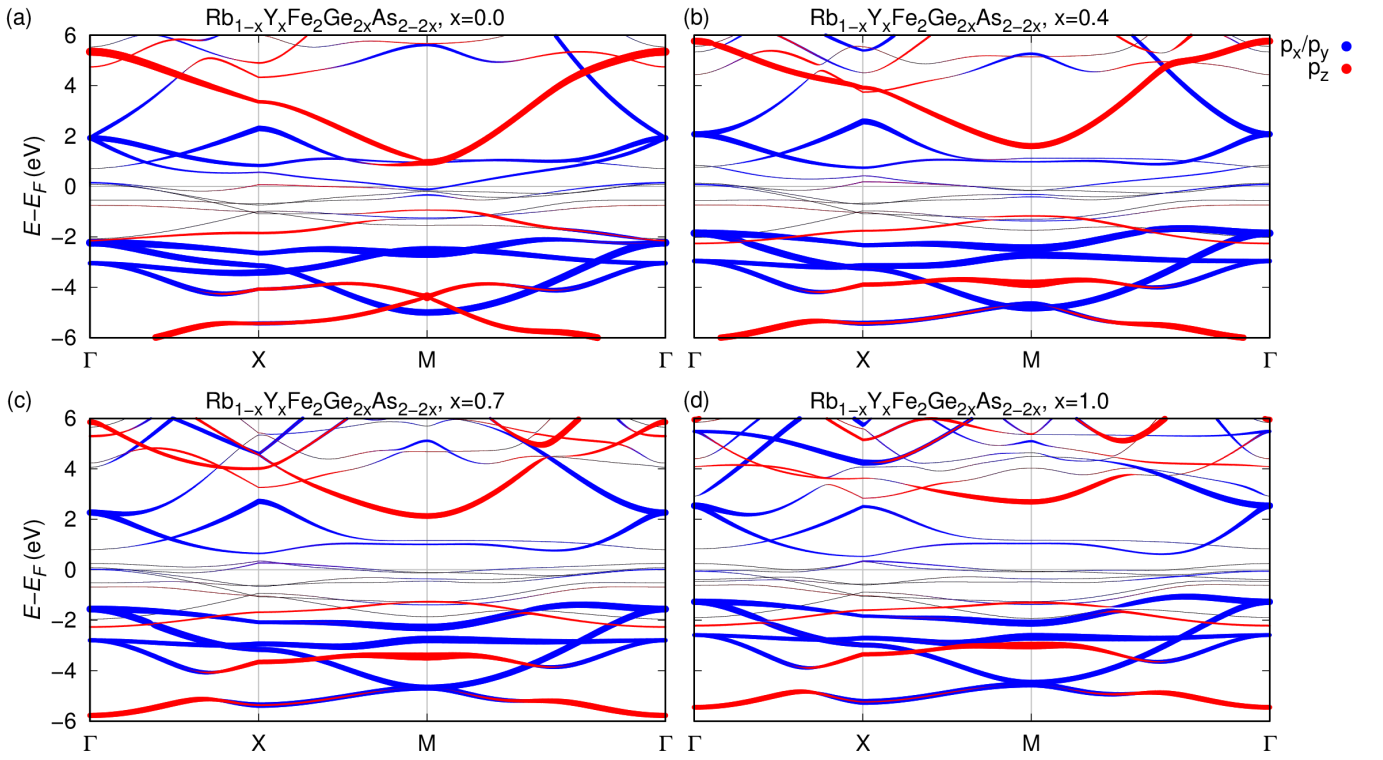
FIG. 9. Electronic bandstructure for the VCA interpolation between $RbFe_2As_2$ and YFe_2Ge_2. Colors indicate the weights of As/Ge $4p$ orbitals.
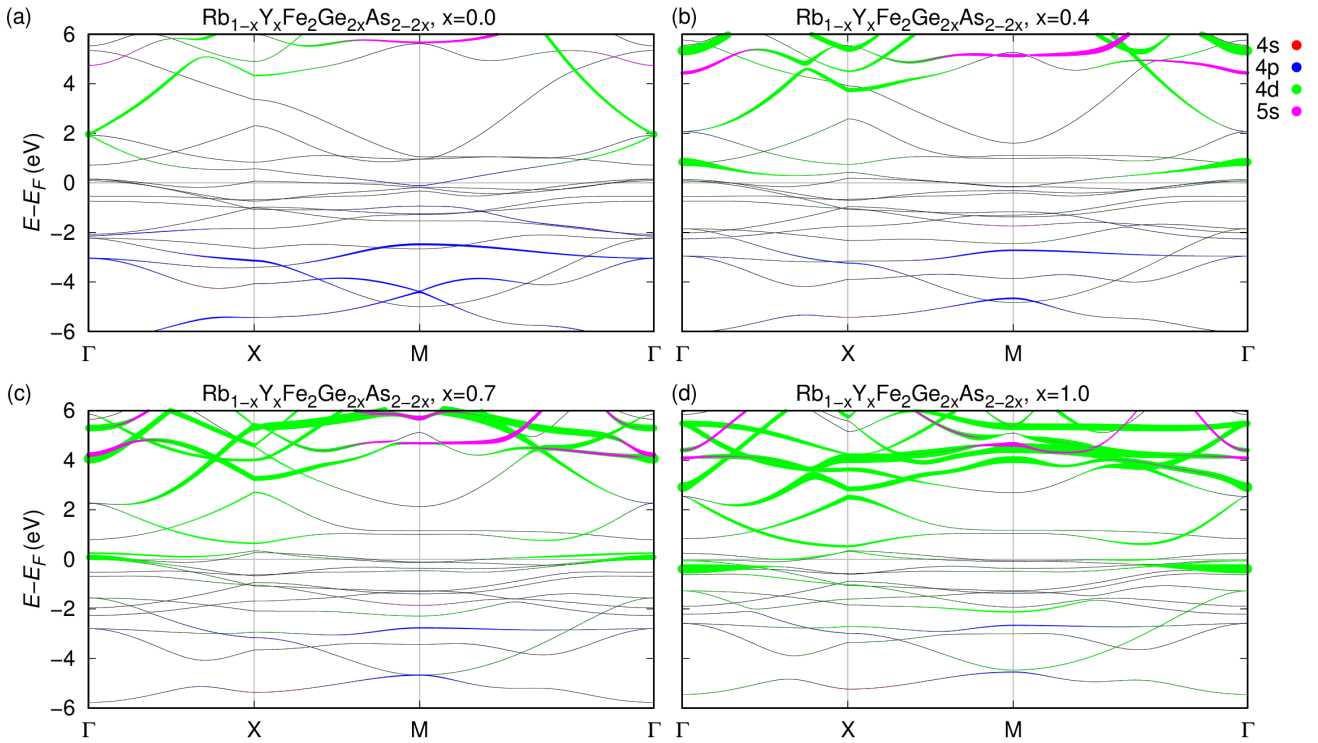
FIG. 10. Electronic bandstructure for the VCA interpolation between $RbFe_2As_2$ and YFe_2Ge_2. Colors indicate the weights of Rb/Y $4s$ and $4d$ orbitals.

* guterding@itp.uni-frankfurt.de

† Present address: Department of Computational and Data Sciences and Computational Materials Science Center, George Mason University, 4400 University Drive, Fairfax, VA 22030

[1] K. Koepernik and H. Eschrig, *Full-potential nonorthogonal local-orbital minimum-basis band-structure scheme*, Phys. Rev. B **59**, 1743 (1999); http://www.FPLO.de

[2] J. P. Perdew, K. Burke, and M. Ernzerhof, *Generalized Gradient Approximation Made Simple*, Phys. Rev. Lett. **77**, 3865 (1996).

[3] G. Wang and X. Shi, *Electronic strctures and magnetism of YM_2Ge_2 (M = Mn-Cu): Ge-height dependent magnetic ordering in YFe_2Ge_2*, Comput. Mater. Sci. **121**, 48 (2016).

[4] A. Subedi, *Unconventional sign-changing superconductivity near quantum criticality in YFe_2Ge_2*, Phys. Rev. B **89**, 024504 (2014).

[5] D. J. Singh, *Superconductivity and magnetism in YFe_2Ge_2*, Phys. Rev. B **89**, 024505 (2014).

[6] I. I. Mazin and D. J. Singh, *Electronic structure and magnetism in Ru-based perovskites*, Phys. Rev. B **56**, 2556 (1997).